

## Degradation of 4-Chlorophenol by Catalytic Ozonation using $\gamma$ - $\text{Al}_2\text{O}_3/\text{TiO}_2$ Supported Manganese Oxides in Aqueous Solution

Lili Qi<sup>1</sup>, Hong You<sup>1,\*</sup>, Zhiwei Zhang<sup>1</sup>, Chunhui Feng<sup>2</sup>, Sjack van Agtmaal<sup>2</sup>

<sup>1</sup> State Key Laboratory of Urban Water Resource and Environment, Harbin Institute of Technology, Harbin, PR China;

<sup>2</sup> Evides Industriewater, Rotterdam, Netherlands

\*E-mail: [youhong@hit.edu.cn](mailto:youhong@hit.edu.cn)

Received: 26 February 2013 / Accepted: 15 March 2013 / Published: 1 April 2013

---

4-Chlorophenol (4-CP) degradation was investigated by catalytic ozonation in the presence of  $\text{MnO}_x/\gamma\text{-Al}_2\text{O}_3/\text{TiO}_2$  (MAT) catalyst. MAT catalyst was synthesized by incipient wetness impregnation using  $\text{Mn}(\text{NO}_3)_2$  as the precursor and  $\gamma\text{-Al}_2\text{O}_3/\text{TiO}_2$  (AT) as the support at pH 6.5-7.5. The as-synthesized samples were characterized by the methods of Brunauer-Emmett-Teller (BET), Fourier transformed infrared (FTIR), Scanning electron microscopy (SEM), X-ray diffractometer (XRD) and X-ray photoelectron spectroscopy (XPS), indicating that the states of manganese oxidation were  $\text{Mn}^{3+}$  and  $\text{Mn}^{4+}$ . MAT catalyst showed more efficient performance with respect to support AT, and 4-CP degradation could achieve up to 69.38% in 10 min. Electron paramagnetic resonance (EPR) as a direct method was used to investigate the generation of hydroxyl radicals showed that MAT catalysts promoted the production of hydroxyl radical and enhanced 4-CP degradation. The addition of *tert*-Butanol (TBA) remarkably inhibited the degradation efficiency of 4-CP by catalytic ozonation, which suggested that 4-CP degradation mainly followed the mechanism of hydroxyl radical oxidation. Increasing the main operating variables, including MAT mass, Mn-supported mass, ozone dose and initial pH, the degradation of 4-CP was promoted.

---

**Keywords:** 4-chlorophenol; catalytic ozonation;  $\text{MnO}_x/\gamma\text{-Al}_2\text{O}_3/\text{TiO}_2$  catalyst; hydroxyl radical; electron paramagnetic resonance; *tert*-butanol.

### 1. INTRODUCTION

As a promising process of AOPs, heterogeneous catalytic ozonation has been focused by researchers in recent years because of no additional chemicals, simple application and high removal efficiency [1,2]. The adsorptive and oxidative prosperities of solid-phase metal oxides with ozone to achieve removal and mineralization of target organics at room temperature. Metals and metal oxides

supported on the supports or minerals are frequently investigated to enhance the recycling ability mechanical ability of the catalyst [2,3].  $\text{Al}_2\text{O}_3$  or  $\text{TiO}_2$ , with the mesoporous structures and large surface areas, is mostly used as active component or catalyst support to reflect the most efficient activity in ozone decomposition in water treatment [4-6].  $\text{Al}_2\text{O}_3/\text{TiO}_2$  (AT) prepared by coprecipitation method as catalyst support has never been reported in catalytic ozonation. As porous and stable materials, AT may be more suitable as support for the uniform dispersion of active components and the presence of more active sites for catalytic reactions. In addition, manganese oxides present particular catalytic performance in catalytic ozonation because of their structural flexibility and wide applications in catalysis [7,8]. It may be feasible that  $\text{Al}_2\text{O}_3/\text{TiO}_2$  as support and  $\text{MnO}_x$  as active component for catalytic ozonation.

4-Chlorophenol (4-CP) is widely generated from a series of industrial processes, such as the manufacturing of plastics, resins, textile, steel and paper, high-temperature coal conversion, and petroleum refining [9]. The reaction rate constant of 4-CP with  $\cdot\text{OH}$  is  $7.6 \times 10^9 \text{ M}^{-1} \cdot \text{s}^{-1}$  [10], whereas that with ozone alone is only  $3.4 \times 10^6 \text{ M}^{-1} \cdot \text{s}^{-1}$  [11], suggesting that 4-CP easily reacts with  $\cdot\text{OH}$ .

In this paper, the performance of  $\text{MnO}_x/\gamma\text{-Al}_2\text{O}_3/\text{TiO}_2$  catalyst in catalytic ozonation was studied.  $\text{MnO}_x$  catalysts were synthesized on the support  $\gamma\text{-Al}_2\text{O}_3/\text{TiO}_2$  via impregnation and were characterized using different techniques. The position and the oxidation state of  $\text{MnO}_x$  within the  $\gamma\text{-Al}_2\text{O}_3/\text{TiO}_2$  structure were discussed. The performance of the as-synthesized and calcined catalysts was compared with  $\gamma\text{-Al}_2\text{O}_3/\text{TiO}_2$  sample. In addition, the primary objectives of this study were to investigate the degradation efficiency of 4-CP using  $\text{MnO}_x/\gamma\text{-Al}_2\text{O}_3/\text{TiO}_2$  in the system of catalytic ozonation, to confirm the reaction mechanism, and to explore the stability of  $\text{MnO}_x/\gamma\text{-Al}_2\text{O}_3/\text{TiO}_2$  catalyst in catalytic ozonation processes.

## 2. EXPERIMENTAL

### 2.1. Catalyst preparation and characterization

The support  $\gamma\text{-Al}_2\text{O}_3/\text{TiO}_2$  (denoted as AT) was prepared by coprecipitation method, and sieved into 40-60 mesh. The carriers were washed three times with distilled water to remove the impurities, dried for 24 h at  $105^\circ\text{C}$ , and calcined at  $500^\circ\text{C}$  for 5 h in an oven (KSW-4D-11B, Harbin Longjiang Electric Furnace Factory, China). The catalysts were synthesized by impregnating the AT support into the  $\text{Mn}(\text{NO}_3)_2$  aqueous solution at pH of 7.5-8.0, and then the slurry were dried at  $100^\circ\text{C}$  for 12 h after being washed several times with deionized water. Afterwards, the samples were calcined at  $500^\circ\text{C}$  for 5 h to gain the  $\text{MnO}_x/\gamma\text{-Al}_2\text{O}_3/\text{TiO}_2$  catalyst (denoted as MAT).

Specific surface area, total pore volume and average pore size of the catalysts were measured by the Brunauer-Emmett-Teller (BET) method. The nitrogen adsorption was performed at  $-200^\circ\text{C}$  by using automatic volumetric adsorption instrument (model Quantachrome Autosorb-1). Fourier transformed infrared (FTIR) analyses were carried out under ambient conditions using a Spectrum 2000-FITR Infrared Spectroscopy (Perkin-Elmer, US). The surface morphology of the prepared catalysts was studied with scanning electron microscopy (SEM; FEI QUANTA 200). The crystal

phases of the catalysts were identified on an X-ray diffractometer (XRD, D/max-rB, Japan) with Cu K $\alpha$  radiation ( $\lambda = 0.15405$  nm). X-ray photoelectron spectroscopy (XPS) was performed with a PHI5700 system equipped with a Mg K $\alpha$  radiation (300 W, 12.5 kV). The C1s peak from the adventitious carbon was used as an internal reference with a binding energy of 284.62 eV. Concerning the oxidation state of manganese, the curve has been adjusted by using a combination of Gaussian-Lorentzian functions.

## 2.2. Analytical method

The pH of the aqueous solution was measured using a PHS-3B analyzer (made in China), with a combination pH electrode (E-201-C, made in China), which was calibrated with standard buffers. The points of zero charge (pzc) of the catalyst were determined by mass titration method. [12] The concentration of catalyst surface hydroxyl groups was determined by the method of acid-base titration. [13]

The concentration of 4-CP was determined by a Shimadzu LC-10AVP HPLC equipped with a COSMOSIL C-18-AR-II column (250, 4.6 mm i.d.). The 4-CP was routinely determined at 280 nm. The mobile phase was an aqueous mixture (70% methanol and 30% water) at a flow rate of 0.1 mL $\cdot$ min $^{-1}$ . The identification of the intermediates by HPLC was performed by comparing the retention time of the peak in the discharged sample with that in the authentic sample. The concentrations of compounds were calculated by using the equations derived from the calibration measurements for the substances. The deviation of HPLC analyses was less than 1%.

Electron paramagnetic resonance (EPR) experiment was conducted for the determination of  $\cdot$ OH generated in the ozonation processes. 5,5-dimethyl-1-pyrrolin-N-oxide (DMPO, Sigma) was adopted as the nitron spin-trapping reagent. The EPR spectrum was measured at room temperature with an EPR spectrometer (Bruker EMX-8/2.7 ESR 8 spectrometer with ER 4102ST cavity) under the following experimental conditions: X-field sweep; center field 3510.00 G; sweep width 100.00 G; static field 3410.00 G; frequency 9.868303 GHz; power 2.25 mW. The sample was scanned and accumulated 8 times for 20.48 s.

## 2.3. Ozonation procedure

The experiments were carried out in a three-phase fluidized bed plexiglass reactor (inner diameter = 50 mm, length = 470 mm and the volume = 1 L). Ozone was produced from pure oxygen (Harbin Gas Co. Ltd., 99.999%, China) through DHX-SS-1G ozone generator (Harbin Jiujiu Electrochemical Engineering Technology Co., Ltd., China), and was subsequently fed into the ozonation reactor through a porous sand plate at the bottom of the reactor to contact thoroughly with the target pollutants (4-CP, 100 mg $\cdot$ L $^{-1}$ ) and the catalysts (AT or MAT). Before the experimental operation, the reactor was pre-ozonated for 5 min and then washed three times with twice-distilled water to exclude possible side effects. Water samples were taken from the tap of the reactor at various times, and the reactions in the samples were stopped by adding a small amount of sodium thiosulphate solution. Then the residual concentration of 4-CP was analyzed by appropriate processes. Adsorption

experiments were carried out in the same reaction conditions using  $N_2$  instead of  $O_3$ . All experiments in this paper were repeated three times to obtain valid data.

### 3. RESULTS AND DISCUSSION

#### 3.1. Catalyst characterization

Given the significant role of heterogeneous catalyst in the process of catalytic ozonation, the surface characteristics of the AT and MAT catalyst were investigated in this study. The main characteristics of the catalysts were summarized in Table 1, including metal content analysis, the pore size distribution and  $pH_{pzc}$  of the samples. Obviously, the Al/Ti ratio remained constant. AT had a high surface area as the support of the as-synthesized MAT sample. Incorporation of manganese oxides on the support resulted in the decrease of the BET surface area and the enhancement of the pore volume, suggesting a porosity gain as a result of thermal treatment.

**Table 1.** Characteristics of the AT and MAT catalysts.

	Mn (wt%)	A/T mass ratio	Mn/AT mass ratio	$S_{BET}$ ( $m^2/g$ )	Pore volume ( $cm^3/g$ )	Average pore diameter (nm)	$pH_{pzc}$
AT	0	0.6865	0	138.1981	0.4096	11.2854	5.49
MAT	17.0832	0.6865	0.6641	105.2637	0.4193	15.2215	6.65

To verify the successful loading of  $MnO_x$  on the AT support, and to characterize the physical properties of the prepared catalyst, SEM, FTIR, XRD, and XPS technologies are used. As shown in the SEM images in Figure 1, significant amount of nanoparticles in diameter of 200-800 nm are observed as compared with the bare AT support, inferring a successful loading of material on the support. FTIR spectra (Figure 2) further verified the appearance of O-Mn-O bonds at the peaks of 764 and 615  $cm^{-1}$ , and the O-H bonds connected with Mn atoms at 1400  $cm^{-1}$ , besides the typical hydroxyl absorption band at 3451.1  $cm^{-1}$  and the adsorbed hydroxyl telescopic vibration absorption band at 1637.3  $cm^{-1}$ . Therefore, the nanoparticles loaded on the AT support in Figure 1b would be  $MnO_x$ , showing a successful loading of the catalyst. The phase composition was further investigated by XRD, as shown in Figure 3. Weak diffraction peaks were observed around 28.8°, 33.5°, 37.5°, 56° and 56.8° which were related to the presence of small amounts of  $MnO_x$ . The peaks near 28.8°, 37.5° and 56.8° were verified for  $MnO_2$  crystal in the form of pyrolusite [14], and the small ones around 33.5° and 56° were attributed to  $Mn_2O_3$  [15]. These results were also in agreement with the XPS results in Figure 4, where the  $Mn2p_{3/2}$  of MAT was found to fit well by two peaks of 641.6 and 642.5 eV, indicating that the oxidation states of manganese were  $Mn^{3+}$  and  $Mn^{4+}$  [16,17]. The distribution of  $Mn^{3+}$  and  $Mn^{4+}$  were 8.41 at% and 2.33 at%. The O 1s spectra of MAT shown in Figure 4 c can be decomposed into three peaks, 529.7 eV (57.79% of total area), 531.5 eV (38.05% of total area), and 533.5 eV (4.04% of total area). The peaks were respectively assigned to lattice oxygen ( $O^{2-}$  or Mn-O-Mn), the oxygen

defect states and the surface-adsorbed molecules ( $\text{OH}^-$ ,  $\text{H}_2\text{O}$  etc.), of which the latter two would play a major role in the catalytic process [18-22].

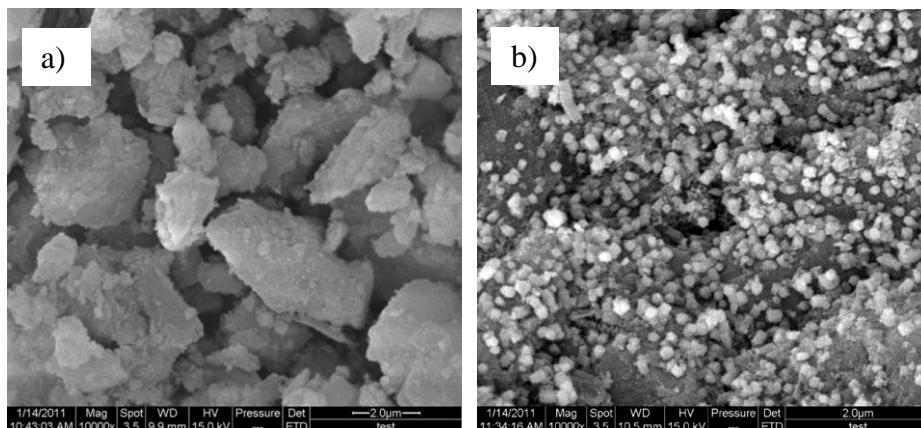


**Figure 1.** SEM images of (a) AT and (b) MAT.

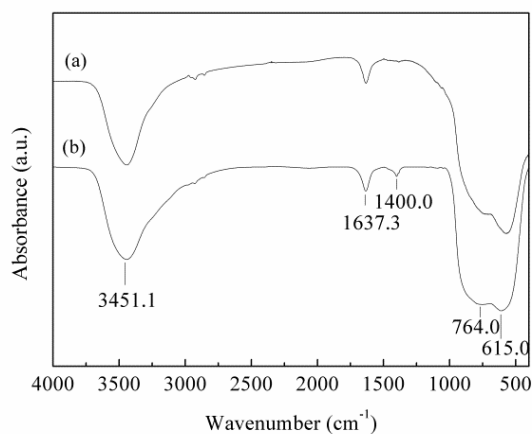


**Figure 2.** FTIR spectra of (a) AT and (b) MAT.

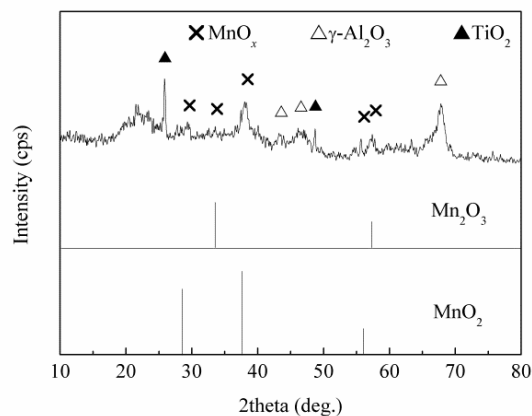


**Figure 3.** XRD patterns of MAT.

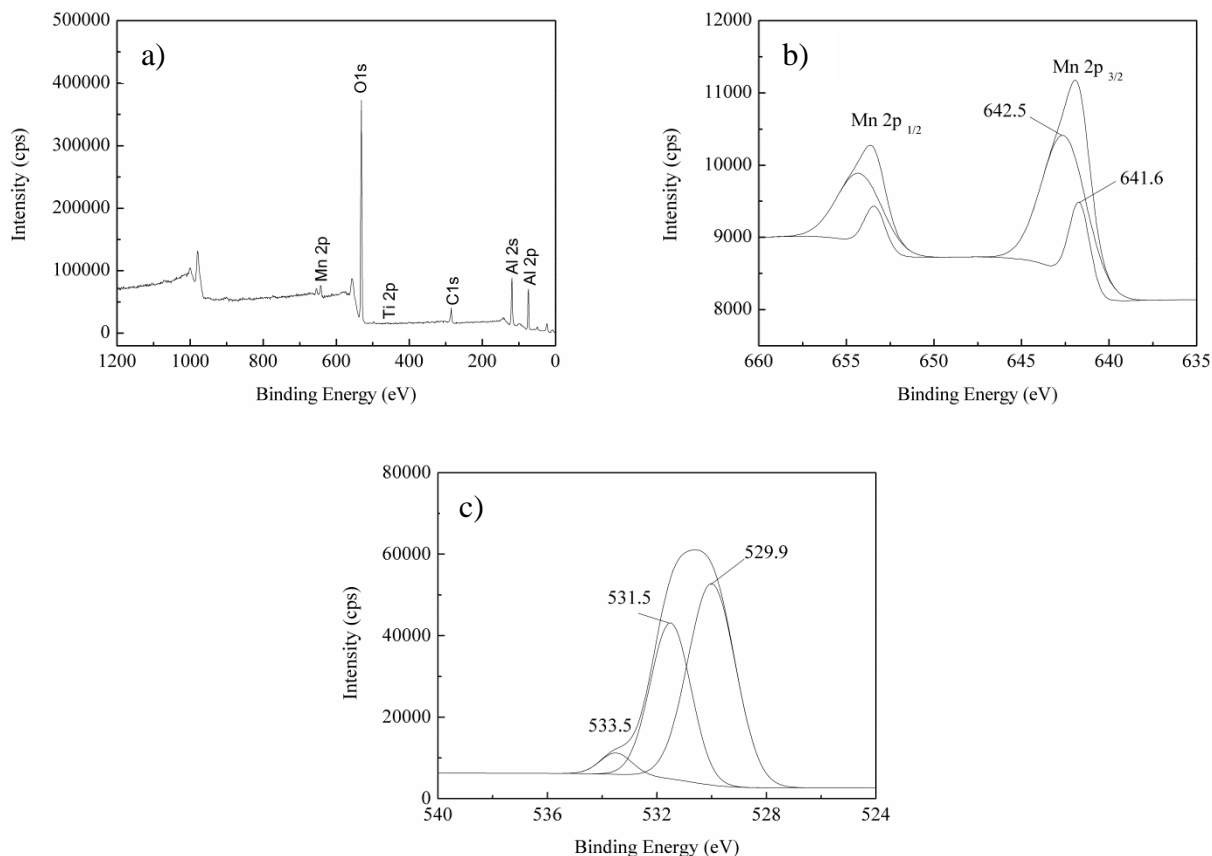


**Figure 4.** XPS spectra analysis of the synthesized MAT catalyst. (a) Wide-range scan, (b) Mn 2p, and (c) O 1s.

The results of MAT characteristics showed that surface hydroxyl groups were developed on the surface of the catalyst, which were considered as one of the crucial factors for the initiation of  $\cdot\text{OH}$  from the decomposition of ozone [23]. In this study, the concentration of the surface hydroxyl groups were measured to be  $1.50126 \times 10^{-6}$  and  $2.17737 \times 10^{-5} \text{ mol} \cdot \text{m}^{-2}$  on the surface of AT and MAT. These hydroxyl groups can adsorb  $\text{H}^+$  and  $\text{OH}^-$  in aqueous solution, and thus adjust the acid-base balance of the solid-liquid interface, as shown in equations (1) and (2):



where MeOH,  $\text{MeOH}_2^+$ , and  $\text{MeO}^-$  represent neutral, protonated, and deprotonated surface hydroxyl groups, respectively. When  $\text{pH} < \text{pH}_{\text{pzc}}$  (6.65), the surface hydroxyl groups on metal oxides are in the protonated form, and when  $\text{pH} > \text{pH}_{\text{pzc}}$ , they are in the deprotonated form [24].

### 3.2 Degradation efficiency of 4-CP in the different processes

To evaluate the catalytic property of the prepared MAT catalyst, 4-CP was adopted as the target contaminant in catalytic ozonation degradation process. As a comparison, ozonation alone and ozonation/AT were also conducted as shown in Figure 5, revealing a great enhancement of the catalytic ozonation degradation of 4-CP by the prepared MAT, which could achieve up to 69.38% in

10 min. It should be noted that if ozone was not introduced, the adsorption on AT or MAT only resulted in a negligible removal of 4-CP, indicating that the removal in the catalytic ozonation was due to degradation but not adsorption. Therefore, the prepared MAT was a good catalyst for the ozonation degradation of 4-CP.

It is well known that ozone reacts in aqueous solution with organic compounds, either by direct reaction (selective one by molecular ozone,  $O_3$ ) or indirect reaction (less selective one involving  $\cdot OH$ , induced by ozone decomposition) [25,26]. In direct reaction, ozone attacks the functional groups with high electron density due to its resonance structures. But due to the electron-withdrawing properties of chlorine atom, 4-CP is hardly to be oxidized by ozonation alone. On the other side,  $\cdot OH$ , being one of the most reactive free radicals and the strongest oxidants towards organic compounds [27,28], has much higher oxidizing potential and thus is more oxidative than molecular ozone. In particular, the reaction rate of  $\cdot OH$  with organic molecules was proved to be in the order of  $10^6$  to  $10^9 M^{-1}\cdot s^{-1}$  [29], while that of ozone is only in the order of  $10^6 M^{-1}\cdot s^{-1}$  [11]. Therefore, it was preliminarily considered that the degradation of 4-CP was mainly attributed to  $\cdot OH$  oxidation in the processes of ozonation, and  $MnO_x$  catalyst might accelerate the decomposition of  $O_3$  molecules to hydroxyl radicals, which could enhance the oxidizing activity of the system from the results of this study. To further confirm and explore the reaction mechanism,  $\cdot OH$  was investigated by EPR technique and by influence of *tert*-butanol (TBA) addition.

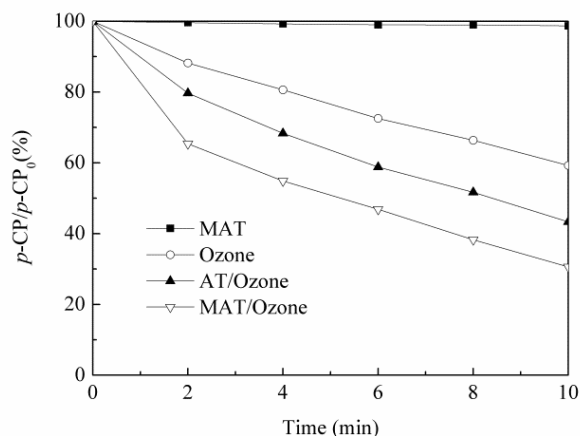


**Figure 5.** Degradation of 4-CP by catalytic ozonation using different Mn-based catalysts. Experimental conditions: temperature  $20 \pm 1^\circ C$ ; initial pH 6.57; initial 4-CP concentration  $100 mg\cdot L^{-1}$ ; catalyst  $2 g\cdot L^{-1}$ ; ozone dose  $1.00 mg\cdot L^{-1}$ .

### 3.3 Mechanism of catalytic ozonation

Spin-trapping/electron paramagnetic resonance (EPR) technique has been accepted to detect  $\cdot OH$  in the previous studies both in ozonation alone and catalytic ozonation [30,31]. Highly reactive hydroxyl radicals are captured by binding spin-trapping reagents DMPO and converted to the corresponding stable spin-adducts DMPO-OH, which can be detected by EPR spectroscopy. The amount of  $\cdot OH$  could be determined from the intensity of the adduct signal by EPR.

As shown in Figure 6, the typical spectrum of DMPO-OH adduct appeared at the initial DMPO concentration of  $100 \text{ mmol}\cdot\text{L}^{-1}$ , which was composed of quartet lines having a peak height ratio of 1:2:2:1 and the parameters are hyperfine constants  $\alpha_{\text{N}} = 1.49 \text{ mT}$ ,  $\alpha_{\text{H}} = 1.49 \text{ mT}$  and  $g$ -value = 2.0055. These parameters corresponded well with those of adducts as demonstrated by the previous reports [32,33]. And importantly, the DMPO-OH adduct signals in the processes of ozonation/AT and ozonation/MAT were stronger than the case of ozonation alone. Therefore, the initiation of  $\cdot\text{OH}$  was consisted in the three processes, and catalytic ozonation could generate a higher concentration of  $\cdot\text{OH}$  under the same experimental conditions compared to ozonation alone due to the introduction of heterogeneous surface, which can significantly affect the ozone decomposition mechanism.

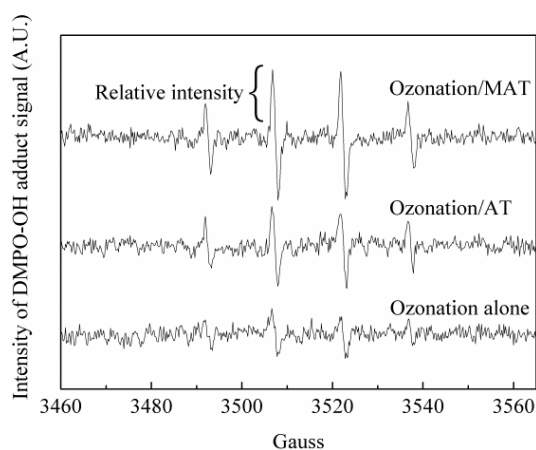


**Figure 6.** Comparison of the intensity of DMPO-OH adduct signal in the different processes. Experimental conditions: temperature  $20 \pm 1^\circ\text{C}$ ; initial pH 6.57; catalyst  $2 \text{ g}\cdot\text{L}^{-1}$ ; ozone applied  $1.00 \text{ mg}\cdot\text{L}^{-1}$ , initial DMPO concentration  $100 \text{ mmol}\cdot\text{L}^{-1}$ .

TBA has a higher reaction rate constant with  $\cdot\text{OH}$  ( $5 \times 10^8 \text{ L}\cdot\text{mol}^{-1}\cdot\text{s}^{-1}$ ) [34], comparing with ozone ( $3 \times 10^{-3} \text{ L}\cdot\text{mol}^{-1}\cdot\text{s}^{-1}$ ) [11]. Therefore, TBA, as a stronger radical scavenger, could react with  $\cdot\text{OH}$  and generate inert intermediates to terminate the  $\cdot\text{OH}$  induced radical chain reactions. [34] According to the report [35], the rate constant of  $\cdot\text{OH}$  with TBA was higher than that with 4-CP by 10 times, which could be considered as a relatively suitable indicator for radical type reaction produced in the systems of catalytic ozonation. The preliminary reaction mechanism of the degradation of 4-CP in the processes of catalytic ozonation was investigated by comparing the presence with the absence of *tert*-butanol (TBA). The experimental results were shown in Figure 7. When  $100 \text{ mg}\cdot\text{L}^{-1}$  TBA was added into the aqueous solution, there were reductions of 14.2% and 42.3% for the degradation efficiency in the processes of ozonation alone and catalytic ozonation at 10 min, respectively. It was clear that the presence of TBA led to the significant decrease of the removal of 4-CP in the processes of ozonation with catalyst or not, suggesting that the 4-CP degradation mainly followed the  $\cdot\text{OH}$  reaction mechanism. The results also stated that the degradation of 4-CP was primarily contributed to  $\cdot\text{OH}$  oxidation in the processes of ozonation alone and ozonation/MAT. It was noted that a certain amount of 4-CP was still removed after the addition TBA attributed to the nonnegligible oxidation of ozone molecules.

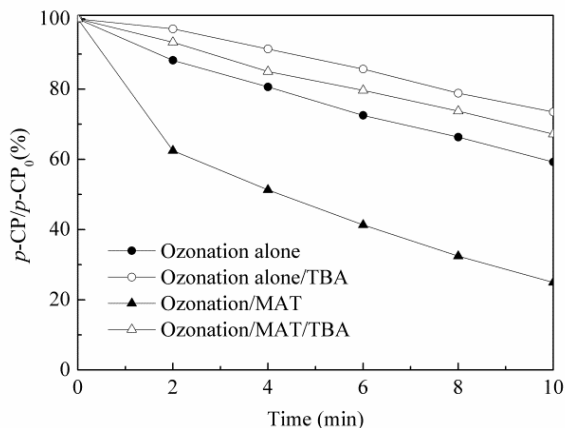


**Figure 7.** Effect of TBA on the degradation of 4-CP. Experimental conditions: temperature  $20 \pm 1^\circ\text{C}$ ; initial pH 6.57; initial 4-CP concentration  $100 \text{ mg}\cdot\text{L}^{-1}$ ; catalyst  $2 \text{ g}\cdot\text{L}^{-1}$ ; ozone applied  $1.00 \text{ mg}\cdot\text{L}^{-1}$ ; TBA  $100 \text{ mg}\cdot\text{L}^{-1}$ .

### 3.4 The influence of variables on 4-CP removal

To further explore the catalytic ozonation process, the effect of different parameters including: catalyst mass, Mn-supported mass, ozone dose and initial pH value for the degradation of 4-CP were studied. Figure 8a showed that the increase of MAT mass from 0 to  $4 \text{ g}\cdot\text{L}^{-1}$  significantly accelerated 4-CP removal due to the fact that more active sites were provided for catalytic reaction and enhanced the heterogeneous catalytic surface, leading to the acceleration of ozone consumption and  $\cdot\text{OH}$  initiation which improves the degradation efficiency of 4-CP.

As shown in Figure 8b, with the increase amount of  $\text{MnO}_x$ , the improvement was further evident. Under the same experimental conditions, ozonation/ $\text{Mn-22.31wt\%/AT}$  system led to 75.05% efficiency of 4-CP degradation at 10 min, indicating an increase of 34.3% compared to the case of ozonation alone. The phenomenon suggested that the presence of AT or MAT had the synergistic effect with ozone, and the modification process could improve the catalytic ozonation activity of Mn-supported catalysts for degradation of 4-CP.

Ozone dose is an important parameter in the system of the heterogeneous catalytic ozonation, which could influence the degradation of the target organic pollutants. As shown in Figure 8c, when  $0.50 \text{ mg/L}$  ozone was applied in the catalytic ozonation process, only 59.46% of 4-CP removal can be observed in 10 min. However, when the ozone dosage increased from 0 to  $2.5 \text{ mg/L}$ , the degradation efficiency of 4-CP was raised up to 92.99%, indicating that the positive effect of increasing ozone dose on 4-CP degradation.

pH value is another important parameter in the processes of ozonation and catalytic ozonation, which could affect the surface properties of catalyst, the generation pathway of hydroxyl radicals and degradation of the pollutants. Figure 8d showed the influence of initial pH value on 4-CP degradation efficiency in both ozonation alone and catalytic ozonation. As shown, the degradation of 4-CP in aqueous solution was greatly enhanced with the increase of the initial pH from 2.57 to 11.13. When pH

values were 2.57, 6.57 and 11.13, the degradation of 4-CP were 33.33%, 40.75% and 73.71% for ozonation alone, respectively. However, the degradation were accordingly 59.49%, 75.05% and 99.77% for catalytic ozonation.

It should be noted that the DMPO-OH adduct signals in different systems were also found to increase with the increase in the degradation rate of 4-CP (data not shown). All these results verified again the hydroxyl radicals reaction mechanism of the ozone with 4-CP in the catalytic process.

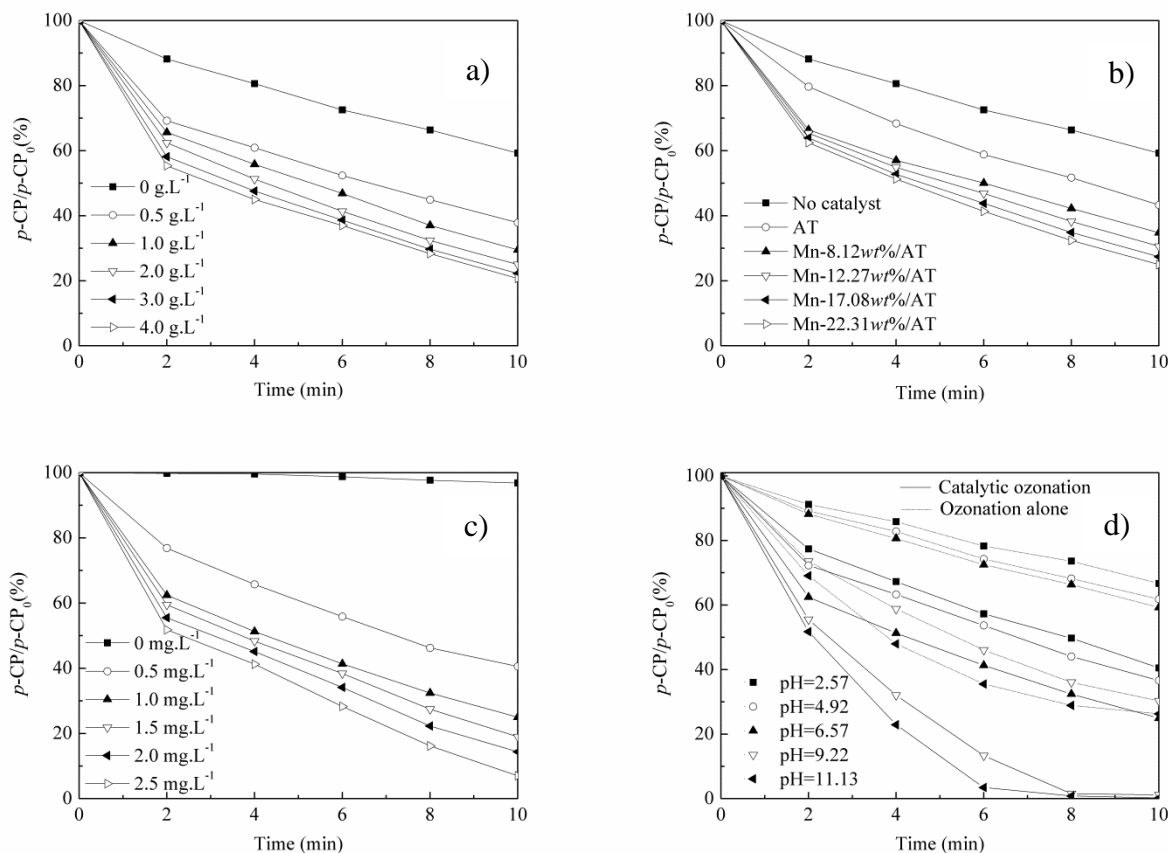


**Figure 8.** Degradation efficiency of 4-CP with different: (a) MAT mass, (b) Mn-supported mass, (c) ozone dose, and (d) pH. Experimental conditions: temperature  $20 \pm 1^\circ\text{C}$ ; initial pH 6.57; initial 4-CP concentration  $100 \text{ mg}\cdot\text{L}^{-1}$ ; ozone applied  $1.00 \text{ mg}\cdot\text{L}^{-1}$ .

The stability and working life of MAT catalyst for the removal of 4-CP was investigated by reusing one sample of catalyst in 10 successive ozonation experiments. The results were shown in Table 2.

**Table 2.** Degradation efficiency of 4-CP under different recycling times.

Recycling times	1	2	3	4	5	6	8	10
4-CP degradation (%)	75.05	74.78	74.37	73.48	72.99	72.25	71.75	70.67

(Experimental conditions: temperature  $20 \pm 1^\circ\text{C}$ ; initial pH 6.57; initial 4-CP concentration  $100 \text{ mg}\cdot\text{L}^{-1}$ ; catalyst  $2 \text{ g}\cdot\text{L}^{-1}$ ; ozone applied  $1.00 \text{ mg}\cdot\text{L}^{-1}$ ; reaction time 10 min.)

The catalyst was collected at the end of each catalytic ozonation process, rinsed with Milli-Q ultrapure water and dried at 50°C. MAT catalyst showed promise for use in water treatment because it retained its catalytic activity for up to 10 successive cycles, still keeping above 70% after 10 min. Therefore, the application of MAT catalyst was feasible in the process of catalytic ozonation for water treatment.

#### 4. CONCLUSION

MnO<sub>x</sub>/γ-Al<sub>2</sub>O<sub>3</sub>/TiO<sub>2</sub> catalysts were successfully synthesized by incipient wetness impregnation method showed the remarkable catalytic activity for degradation of 4-chlorophenol. The characterizations of the Mn-catalysts revealed that Mn were distributed on the surface of support γ-Al<sub>2</sub>O<sub>3</sub>/TiO<sub>2</sub> in the oxidation states of Mn<sup>3+</sup> and Mn<sup>4+</sup>. The presence of MnO<sub>x</sub>/γ-Al<sub>2</sub>O<sub>3</sub>/TiO<sub>2</sub> catalysts could improve the degradation of 4-chlorophenol for catalytic ozonation, as compared with ozonation alone and ozonation/γ-Al<sub>2</sub>O<sub>3</sub>/TiO<sub>2</sub>. The presence of *tert*-butanol had intense inhibited effect on MnO<sub>x</sub>/γ-Al<sub>2</sub>O<sub>3</sub>/TiO<sub>2</sub> for catalytic ozonation, and more hydroxyl radicals were detected in the presence of MnO<sub>x</sub>/γ-Al<sub>2</sub>O<sub>3</sub>/TiO<sub>2</sub> than that of in the systems of ozonation alone and ozonation/γ-Al<sub>2</sub>O<sub>3</sub>/TiO<sub>2</sub> by spin-trapping/electron paramagnetic resonance determination. The degradation of 4-CP by catalytic ozonation of MAT was proved to mainly follow the indirect reaction with ·OH, which was decomposed by ozone and was further enhanced by MnO<sub>x</sub>/γ-Al<sub>2</sub>O<sub>3</sub>/TiO<sub>2</sub> catalyst introduction. Moreover, the removal effectiveness of 4-CP was also enhanced with the increase of MAT mass, Mn-supported mass, ozone dose and initial pH value.

#### ACKNOWLEDGEMENT

Research supported via funding coming from the Sino-Dutch Research Program for industrial waste water treatment, water reuse and Zero Liquid Discharge. A program established in November 2011 in Xi'An via a cooperation between Evides (Rotterdam, the Netherlands), University of Delft (Delft, the Netherlands), PEAS (Xi'An, China) and HIT (Harbin, China).

#### References

1. F.J. Beltran, P. Pocostales, P.M. Alvarez and F. Lopez-Pineiro, *Appl. Catal. B*, 92 (2009) 262
2. F. Delanoë, B. Acedo, N. Karpel Vel Leitner and B. Legube, *Appl. Catal. B*, 29 (2001) 315
3. R. Rosal, M.S. Gonzalo, A. Rodríguez, J.A. Perdigón-Melón and E. García-Calvo, *Chem. Eng. J.*, 165 (2010) 806
4. C.Y. Chang, M.H. Yuan, J.L. Shie, C.C. Chang, J.H. Chen and W.T. Tsai, *J. Hazard. Mater.*, 175 (2010) 809
5. H. Hidaka, T. Oyama, I. Yanagisawa, M. Takeuchi, T. Koike and N. Serpone, *Appl. Catal. B*, 91 (2009) 242
6. S.M. Avramescu, C. Bradu, I. Udrea, N. Mihalache and F. Ruta, *Catal. Commun.*, 9 (2008) 2386
7. A.M. Zhang, Y.M. Dong, H.X. Yang, K. He and S.Q. Song, *Appl. Catal. B*, 85 (2009) 155
8. X.Y. Wang, Q. Kang and D. Li, *Appl. Catal. B*, 86 (2009) 166
9. M. Gomez, M.D. Murcia, N. Christofi, E. Gomez and J.L. Gomez, *Chem. Eng. J.*, 158 (2010) 120

10. G.V. Buxton, C.L. Greenstock, W.P. Helman and A.B. Ross, *J. Phys. Chem. Ref. Data*, 17 (1988) 513
11. E.V. Potapenko and P.Y. Andreev, *Petrol. Chem+*, 52 (2012) 113
12. T. Preocanin and N. Kallay, *Croat. Chem. Acta*, 79 (2006) 95
13. H. Tamura, A. Tanaka, K. Mita and R. Furuichi, *J. Colloid Interf. Sci*, 209 (1999) 225
14. F. Arena, G. Trunfio, J. Negro, B. Fazio and L. Spadaro, *Chem. Mater.*, 19 (2007) 2269
15. S.C. Kim and W.G. Shim, *Appl. Catal. B*, 98 (2010) 180
16. M.I. Masaya Chigane, *J. of Electrochem. Soc.*, 147 (2000) 2246
17. M. Liu, G.J. Zhang, Z.R. Shen, P.C. Sun, D.T. Ding and T.H. Chen, *Solid State Sci.*, 11 (2009) 118
18. N. Han, X. Wu, L. Chai, H. Liu and Y. Chen, *Sens. Actuators, B*, 150 (2010) 230
19. X. Cao, N. Wang, L. Wang, C.P. Mo, Y.J. Xu, X.L. Cai and L. Guo, *Sens. Actuators, B*, 147 (2010) 730
20. M. Ramstedt, A. Shchukarev and S. Sjoberg, *Surf. Interface. Anal.*, 34 (2002) 632
21. H.W. Nesbitt and D. Banerjee, *Am. Mineral.*, 83 (1998) 305
22. S. Ardizzone, C.L. Bianchi and D. Tirelli, *Colloids Surf., A*, 134 (1998) 305
23. W. Li, Z. Qiang, T. Zhang and F. Cao, *Appl. Catal. B*, 113 (2012) 290
24. L. Zhao, Z.Z. Sun, J. Ma and H.L. Liu, *Environ. Sci. Technol.*, 43 (2009) 2047
25. B. Kasprzyk-Hordern, *Appl. Catal. B*, 46 (2003) 639
26. J. Nawrocki, B. Kasprzyk-Hordern, P. Andrzejewski, A. Dabrowska and K. Czaczyk, *Appl. Catal. B*, 51 (2004) 51
27. J. Peral, E. Piera, J.C. Calpe, E. Brillas and X. Domenech, *Appl. Catal. B*, 27 (2000) 169
28. A.H. Lv, C. Hu, Y.L. Nie and J.H. Qu, *Appl. Catal. B*, 117 (2012) 246
29. R. Rosal, M.S. Gonzalo, A. Rodríguez and E. García-Calvo, *J. Hazard. Mater.*, 183 (2010) 271
30. F.J. Beltran, F.J. Rivas and R. Montero-de-Espinosa, *Appl. Catal. B*, 39 (2002) 221
31. B.S. Kim, H. Fujita, Y. Sakai, A. Sakoda and M. Suzuki, *Water Sci. Technol.*, 46 (2002) 35
32. H. Utsumi, M. Hakoda, S. Shimbara, H. Nagaoka, Y.S. Chung and A. Hamada, *Water Sci. Technol.*, 30 (1994) 91
33. H. Xiao, R.P. Liu, X. Zhao and J.H. Qu, *J. Mol. Catal. A: Chem.*, 286 (2008) 149
34. B. Langlais, D.A. Reckhow and D.R. Brank, *Ozone in Water Treatment: Application and Engineering*, Lewis, Michigan (1991)
35. Y.Z. Pi, L.S. Zhang and J.L. Wang, *J. Hazard. Mater.*, 141 (2007)